RESEARCH ARTICLE

Figures and figure supplements

Structure and mechanism of a phage-encoded SAM lyase revises catalytic function of enzyme family

Xiaohu Guo *et al*

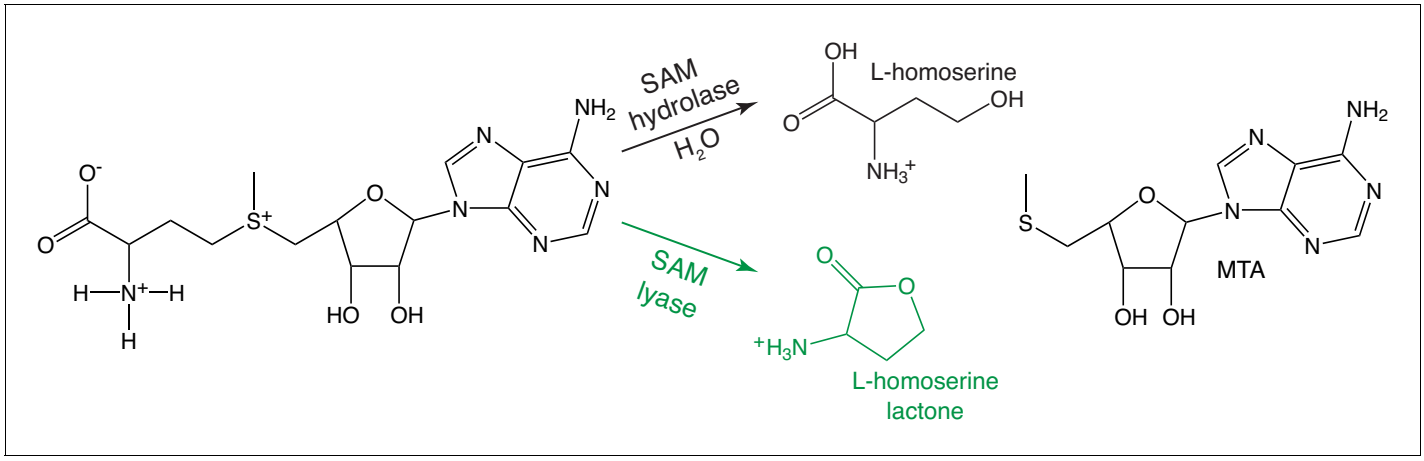

Figure 1. SAMase reaction. Top: Hypothetical S-adenosyl methionine (SAM) hydrolase reaction previously suggested to be catalyzed by T3 SAMase. Bottom, green: SAM lyase reaction shown in this study to be catalyzed by all tested bacteriophage SAMases.

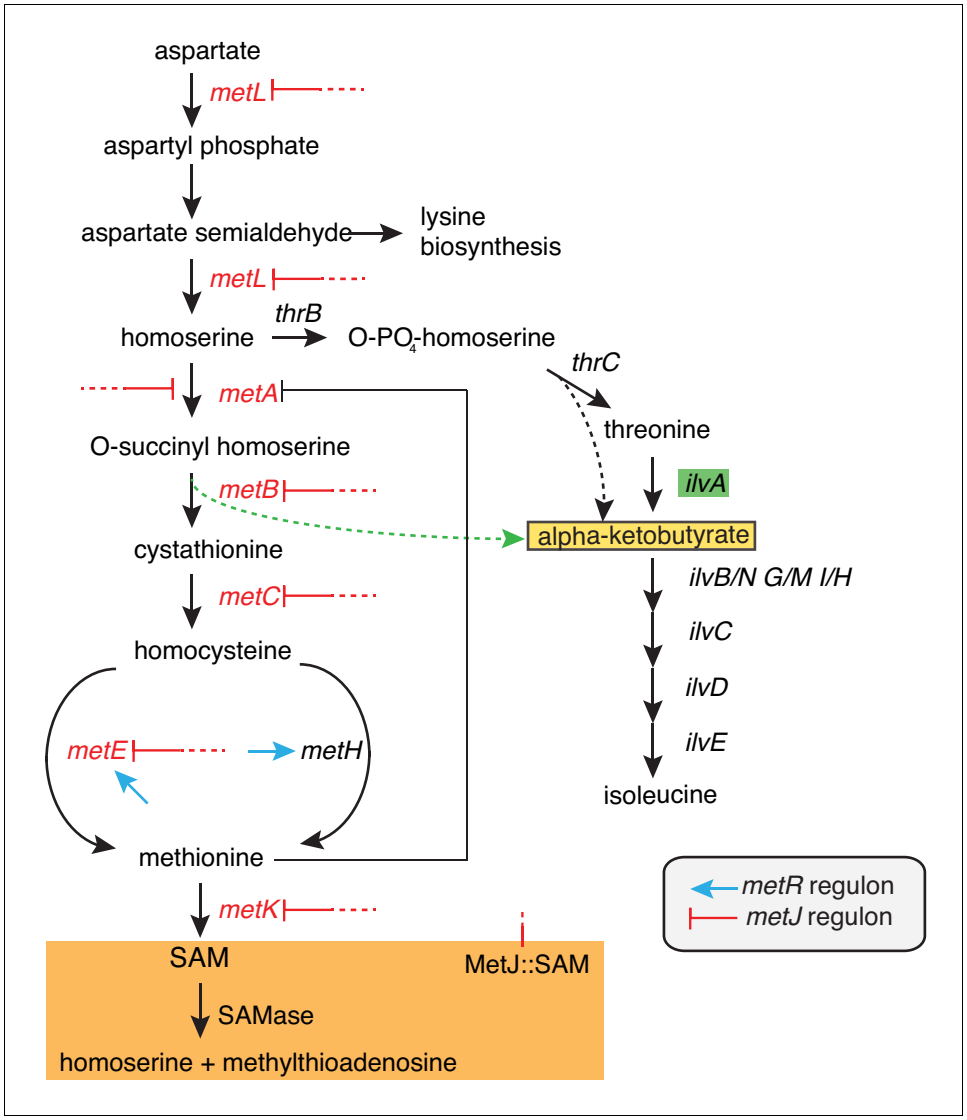

Figure 1—figure supplement 1. Proposed mechanism of rescue of an *ilvA* auxotrophic mutant by SAMases (***Jerlström Hultqvist et al., 2018***). Expression of enzymes in the methionine synthesis pathway is repressed by MetJ in complex with S-adenosyl methionine (SAM). SAM degradation leads to increased expression of the enzymes in the *metJ* regulon. At high expression level, the promiscuous function of MetB, production of alpha-ketobutyrate from O-succinyl homoserine (green arrow), provides rescue of isoleucine biosynthesis.

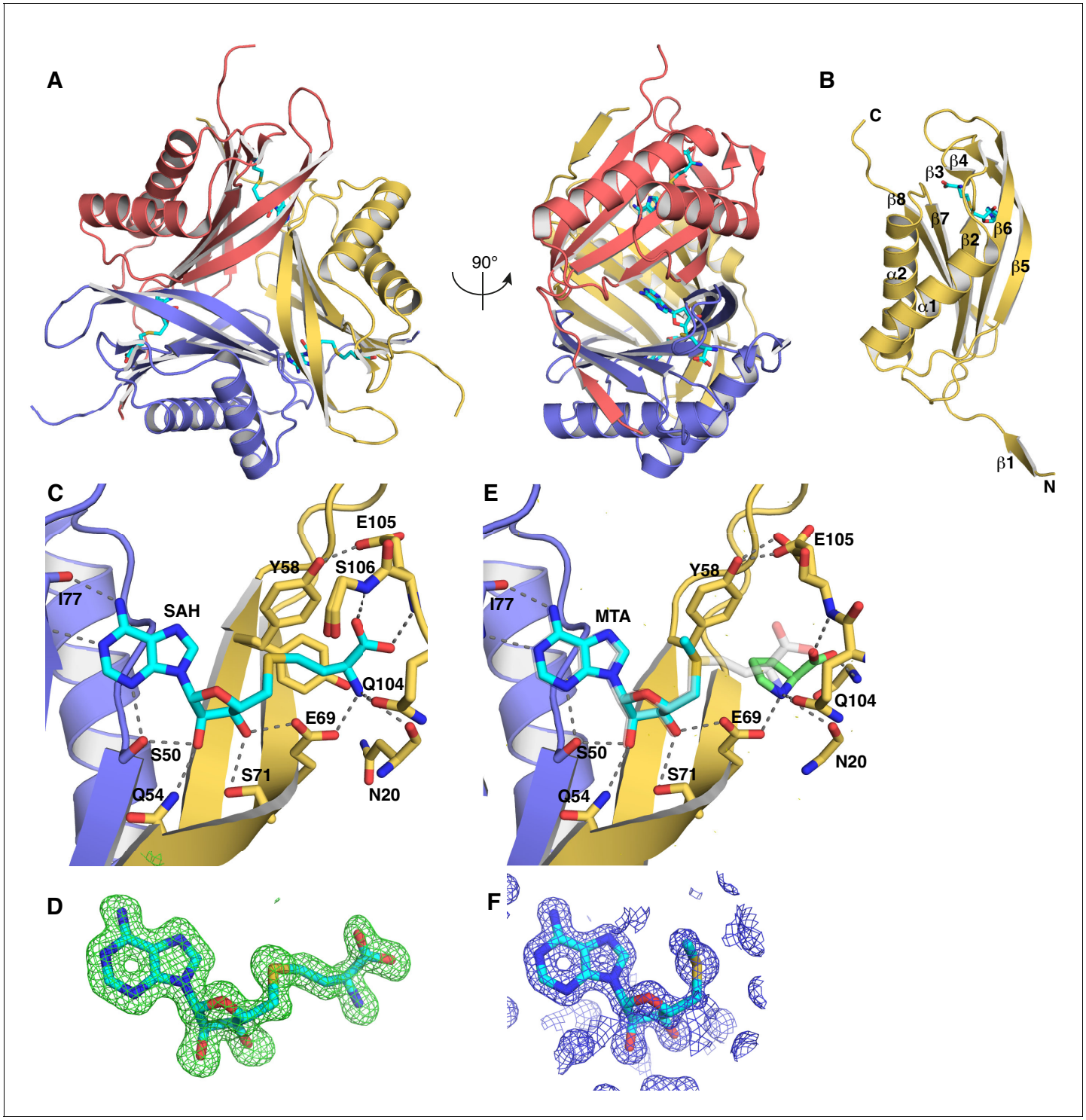

Figure 2. Structure of SAMase Svi3-3. (**A**) Structure of the Svi3-3 trimer in complex with S-adenosyl homocysteine (SAH). (**B**) Monomer structure of Svi3-3. (**C**) Interactions of SAH (cyan sticks) at the trimer interface, (**D**) F_o–F_c omit map for SAH contoured at three sigma. (**E**) 5'-Methyl-thioadenosine (MTA; cyan sticks) and Pro (green sticks), overlay of SAH is shown in transparent light gray sticks. (**F**) Unbiased Arcimboldo (***Rodríguez et al., 2009***) electron density map for MTA bound to Svi3-3, contoured at two sigma (0.39 $e^-/Å^3$).

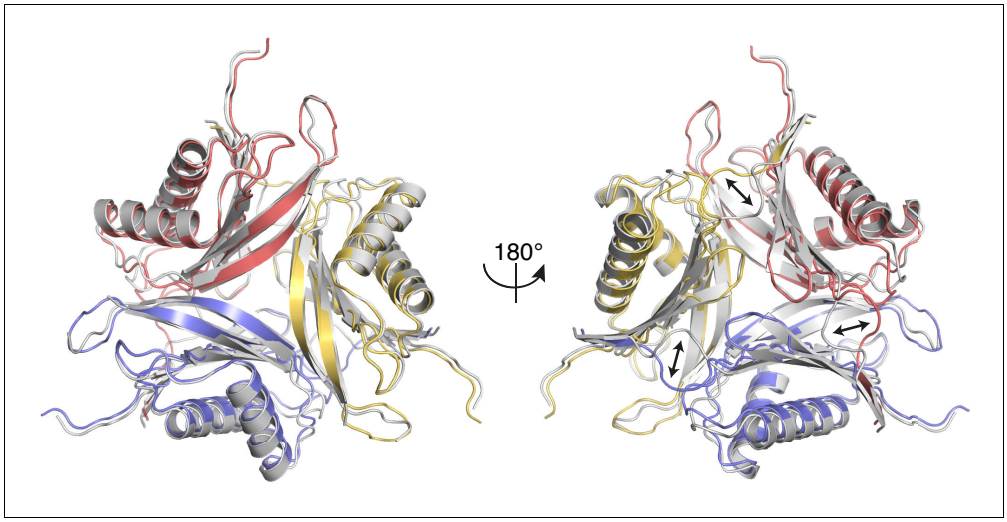

Figure 3. Comparison of the apo structure of Svi3-3 (gray) and the 5′-methyl-thioadenosine (MTA) complex structure (colored as in Figure 2A, transparent). Arrows indicate conformational differences between the N-terminal regions in the two structures.

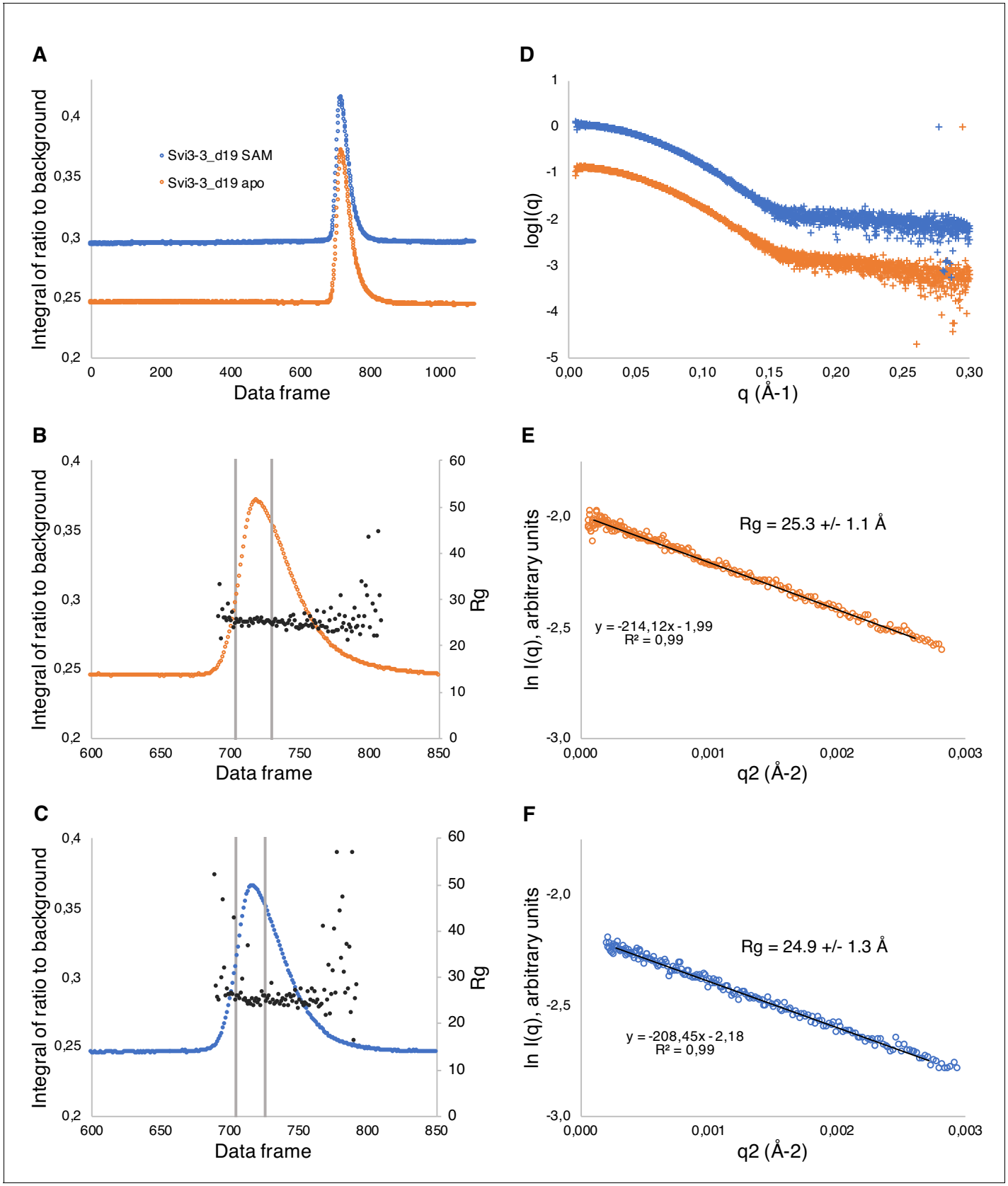

Figure 3—figure supplement 1. Size-exclusion chromatography coupled to small angle X-ray scattering (SEC-SAXS) of Svi3-3. (**A**) Overlay of signal plots from SEC-SAXS of Svi3-3 in the presence and absence of 5 mM S-adenosyl methionine (SAM; plotted with an offset of 0.05 for clarity). (**B and C**)

Figure 3—figure supplement 1 continued on next page

Figure 3—figure supplement 1 continued

Zoom in of signal plot for Svi3-3 apo (**B**) and Svi3-3 in the presence of SAM (**C**). Black markers indicate the radii of gyration (R_g) calculated from the individual scattering curves. Gray bars indicate the data frames used for further analysis. (**D**). Scattering curves for Svi3-3 in the presence and absence of SAM. Colors as in A. The blue curve is for clarity plotted with an offset of +1. (**E**). Guinier plot for Svi3-3 apo. (**F**). Guinier plot for Svi3-3 in the presence of SAM.

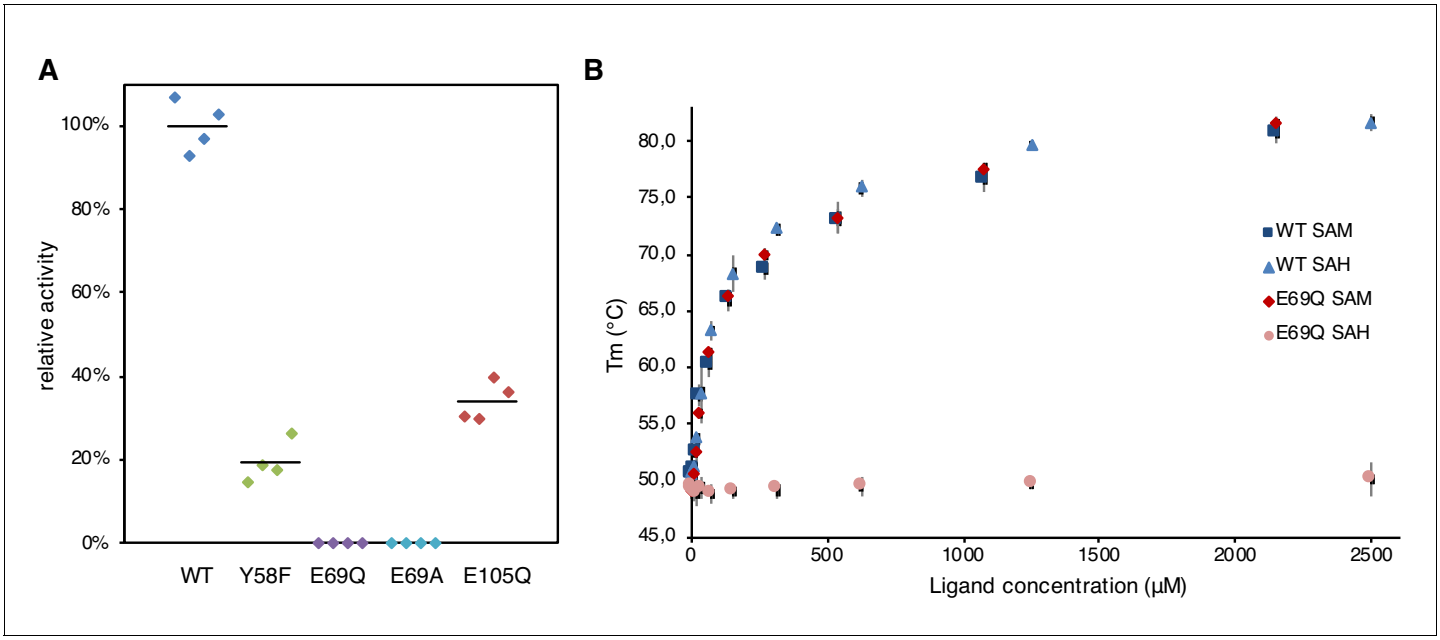

Figure 4. Svi3-3 assays. (**A**) Relative enzymatic activity of Svi3-3 variants. The data points are based on technical duplicates from two different protein purifications, where activity is related to wild type (WT) purified at the same time and the average is represented by a black line. (**B**) Differential scanning fluorimetry (DSF) data for Svi3-3 variants with different concentrations of S-adenosyl methionine (SAM) and S-adenosyl homocysteine (SAH). Error bars correspond to ±1 standard deviation based on triplicate data.

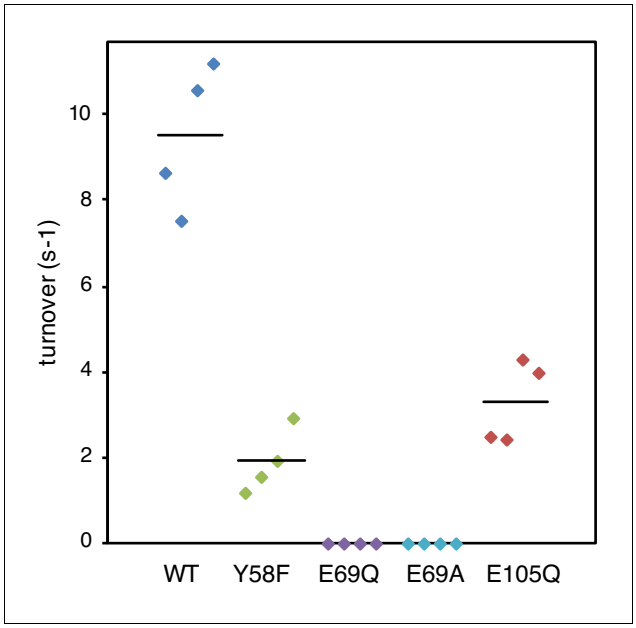

Figure 4—figure supplement 1. Absolute enzymatic activity of Svi3-3 variants. Data is from technical duplicates from two different protein purifications (ordered from left to right) with the average represented by a black line. Calculated average activities ±1 standard deviation: wild type (WT): 9.5 ± 1.7 s^{-1}, Y58F: 1.9 ± 0.7 s^{-1}, E69Q: 0.002 ± 0.0006 s^{-1}, E69A: 0.007 ± 0.0016 s^{-1}, E105Q: 3.3 ± 0.99 s^{-1}.

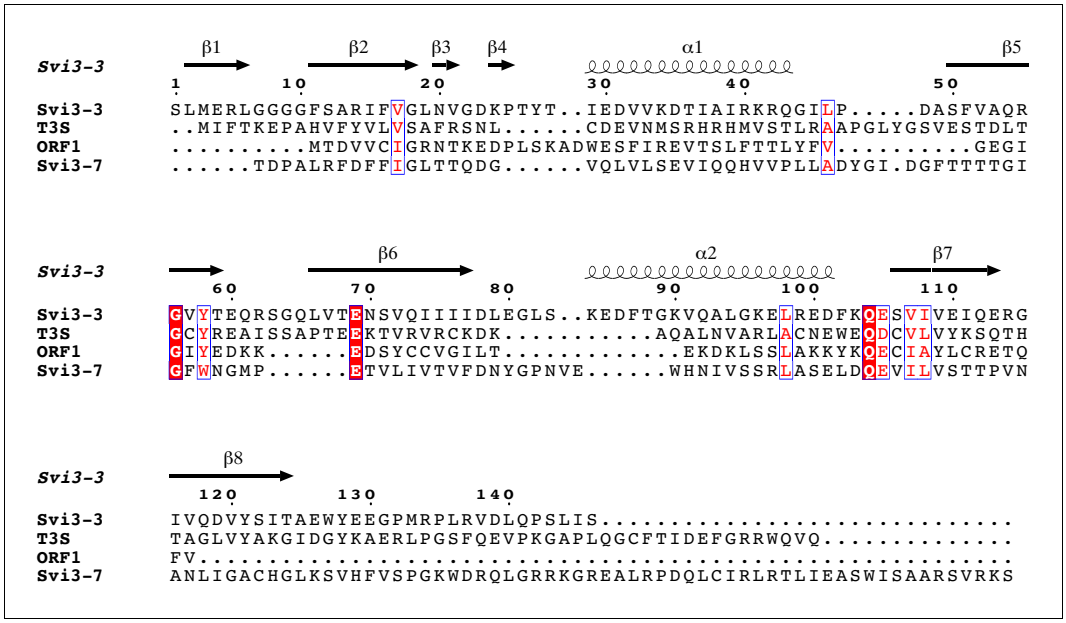

Figure 5. Structure-guided sequence alignment of SAMases with demonstrated activity (***Jerlström Hultqvist et al., 2018***). Secondary structure of Svi3-3 is displayed above the alignment. Red boxes with white letters indicate conserved residues and red letters in white boxes show conservatively substituted residues. Figure was prepared using ESPript (***Gouet et al., 2003***).

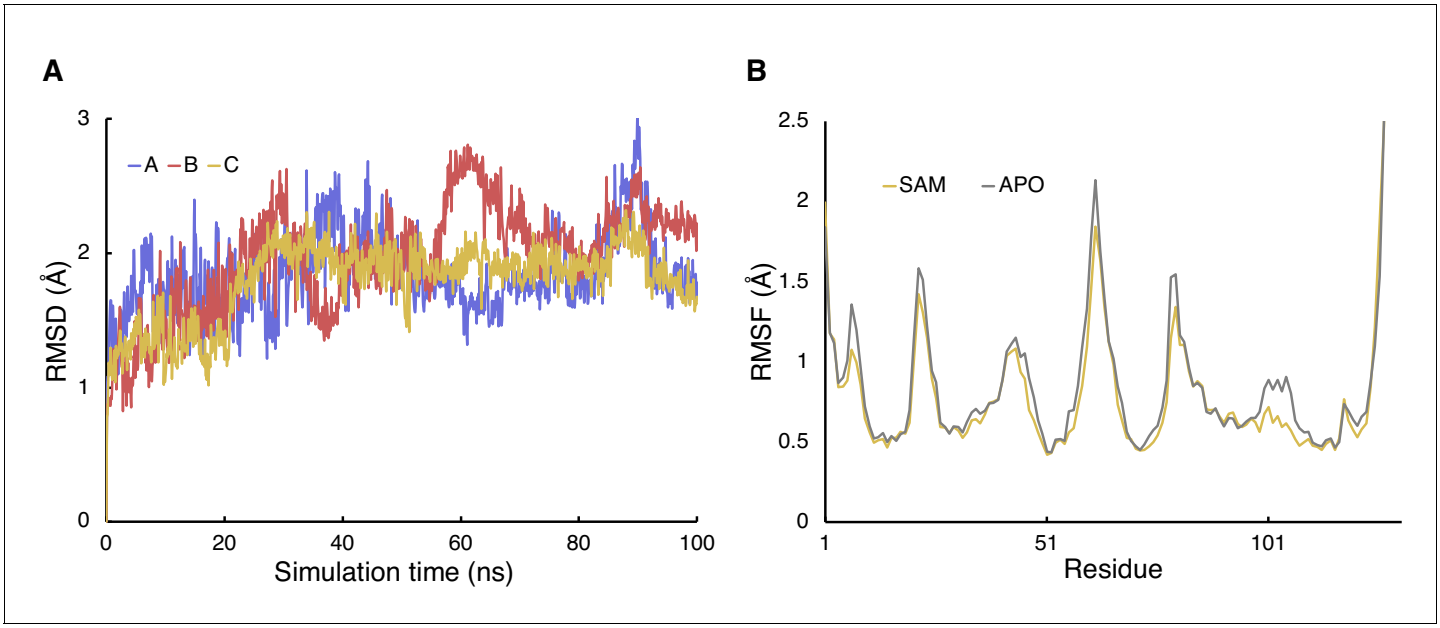

Figure 6. Molecular dynamics (MD) simulations of Svi3-3. (**A**) Time evolution of root mean square deviation (RMSD) to the Svi3-3 crystal structure for each monomer during the 100 ns MD simulation in the presence of S-adenosyl methionine (SAM). (**B**) Average backbone root mean square fluctuation (RMSF) over 100 ns MD simulation of apo Svi3-3 and its complex with SAM. The largest difference is seen for active-site residues 104–106.

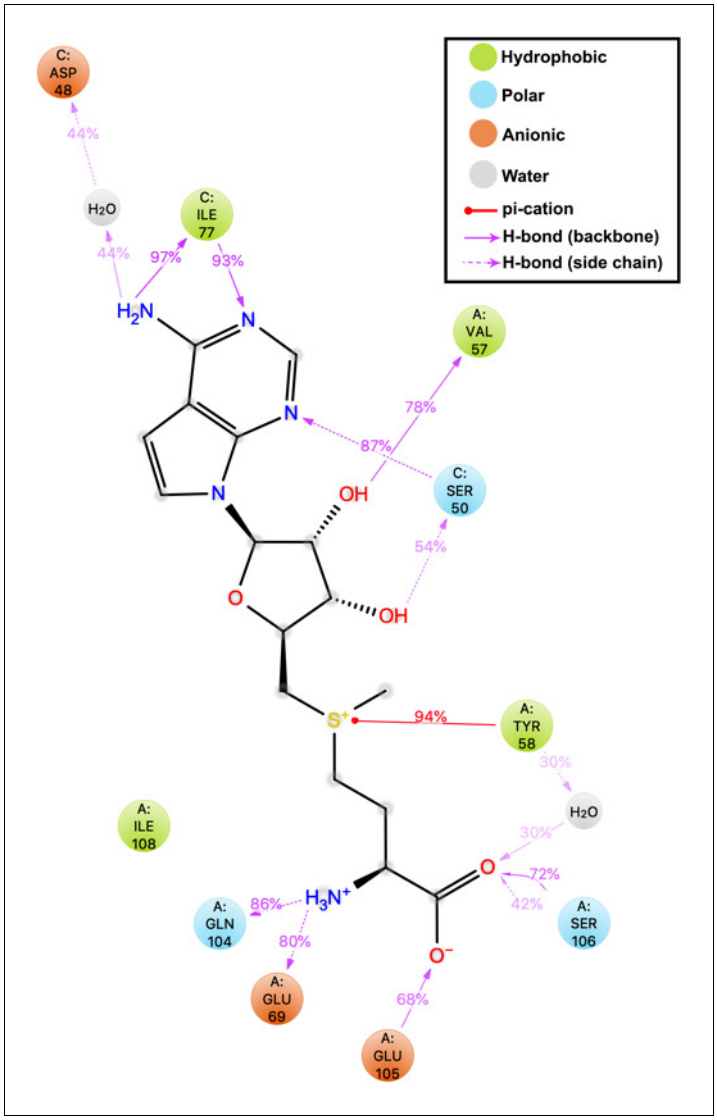

Figure 6—figure supplement 1. Protein–ligand interactions obtained from 100 ns molecular dynamics (MD) simulations illustrating the percentage of interaction from the total simulation time.

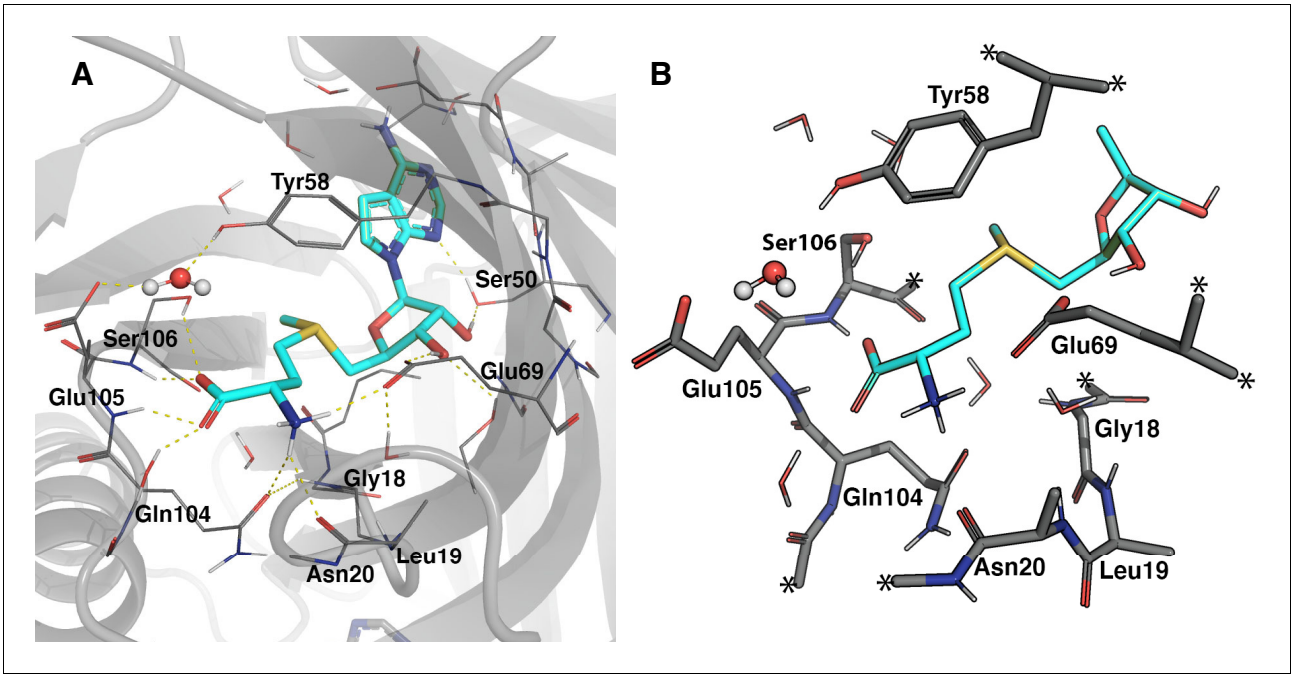

Figure 6—figure supplement 2. Active-site structure of Svi3-3 as observed from MD simulations. (**A**) Snapshot from 100 ns molecular dynamics (MD) simulation illustrating the dominant interactions for the methionine part of the ligand in the active site. (**B**) Density functional theory (DFT) cluster model utilized for the DFT calculations. Atoms marked with an asterisk are kept fixed during the calculations.

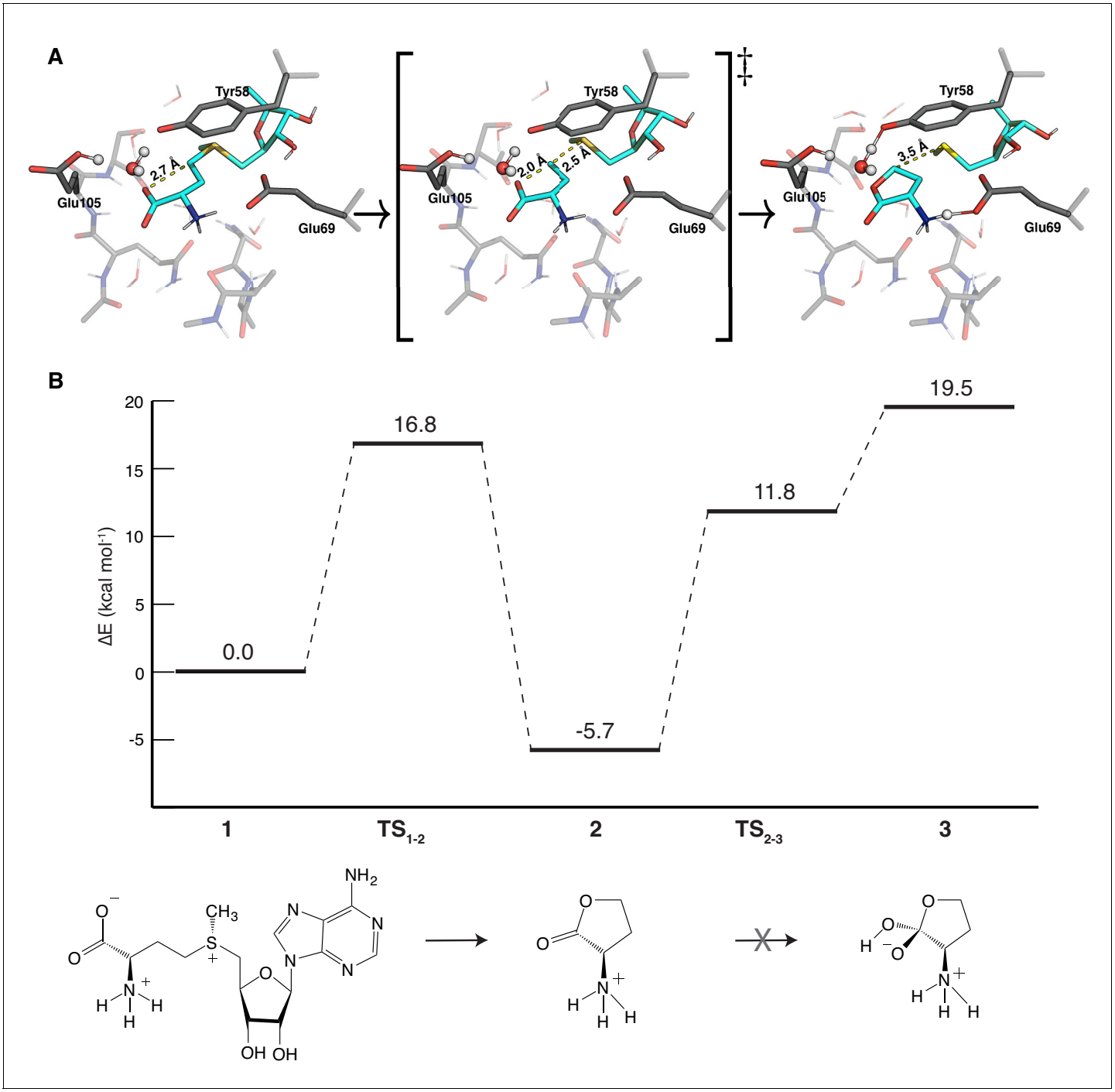

Figure 7. Density functional theory (DFT) calculations on the S-adenosyl methionine (SAM) lyase reaction of Svi3-3. (**A**) Optimized DFT structures for the reactant (left), transition (middle), and product (right) state in the SAM lyase reaction mechanism. (**B**) Calculated free energy profiles for reactant (1), transition state (1–2) and product state (2) for the SAM lyase reaction mechanism. Further conversion from homoserine lactone (2) to the tetrahedral intermediate (3) that would form homoserine is not supported by the high DFT energies.

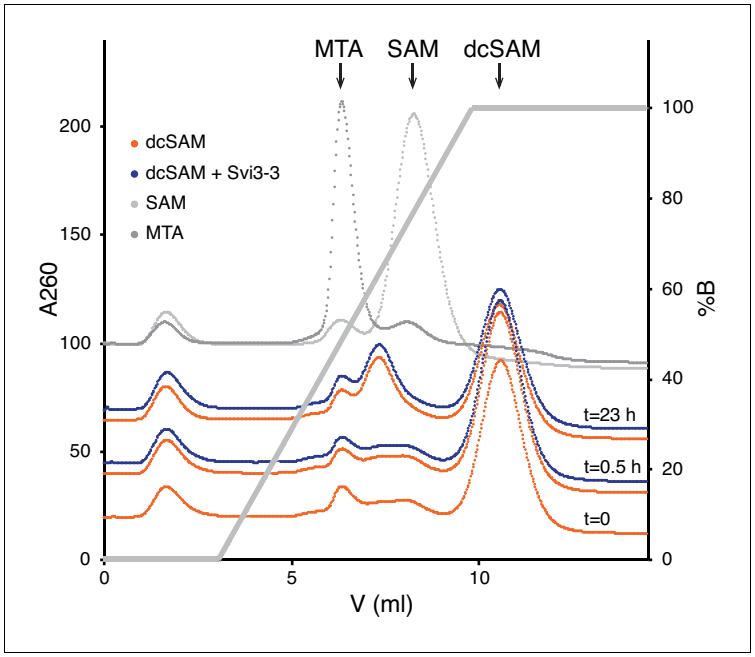

Figure 8. Representative chromatogram from ion exchange chromatography of decarboxylated S-adenosyl methionine (dcSAM) reactions and controls. 0.32 mM dcSAM mix (77% dcSAM) was incubated ± Svi3-3 for 0–23 hr.

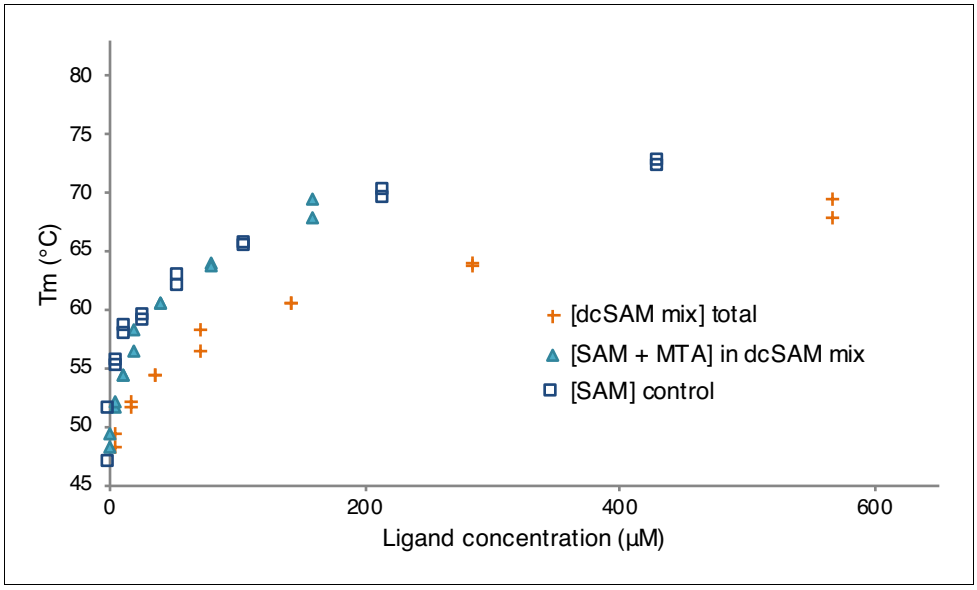

Figure 8—figure supplement 1. Differential scanning fluorimetry (DSF) duplicate data for Svi3-3 in the presence of different concentrations of decarboxylated S-adenosyl methionine (dcSAM) mix (72% dcSAM, 28% S-adenosyl methionine [SAM] + 5'-methyl-thioadenosine [MTA], orange plus signs) and SAM (open blue squares). The dcSAM mix T_m values are also plotted as function of the concentration of SAM + MTA in the mix (cyan triangles). If dcSAM would bind to Svi3-3 and increase its thermal stability to the same extent as SAM and MTA, the orange plus signs and blue squares would overlap. If dcSAM would at all contribute to thermal stabilization, the cyan triangles would be above the open blue squares. The data indicate that dcSAM in a mixture with 28% SAM + MTA does not bind to Svi3-3.

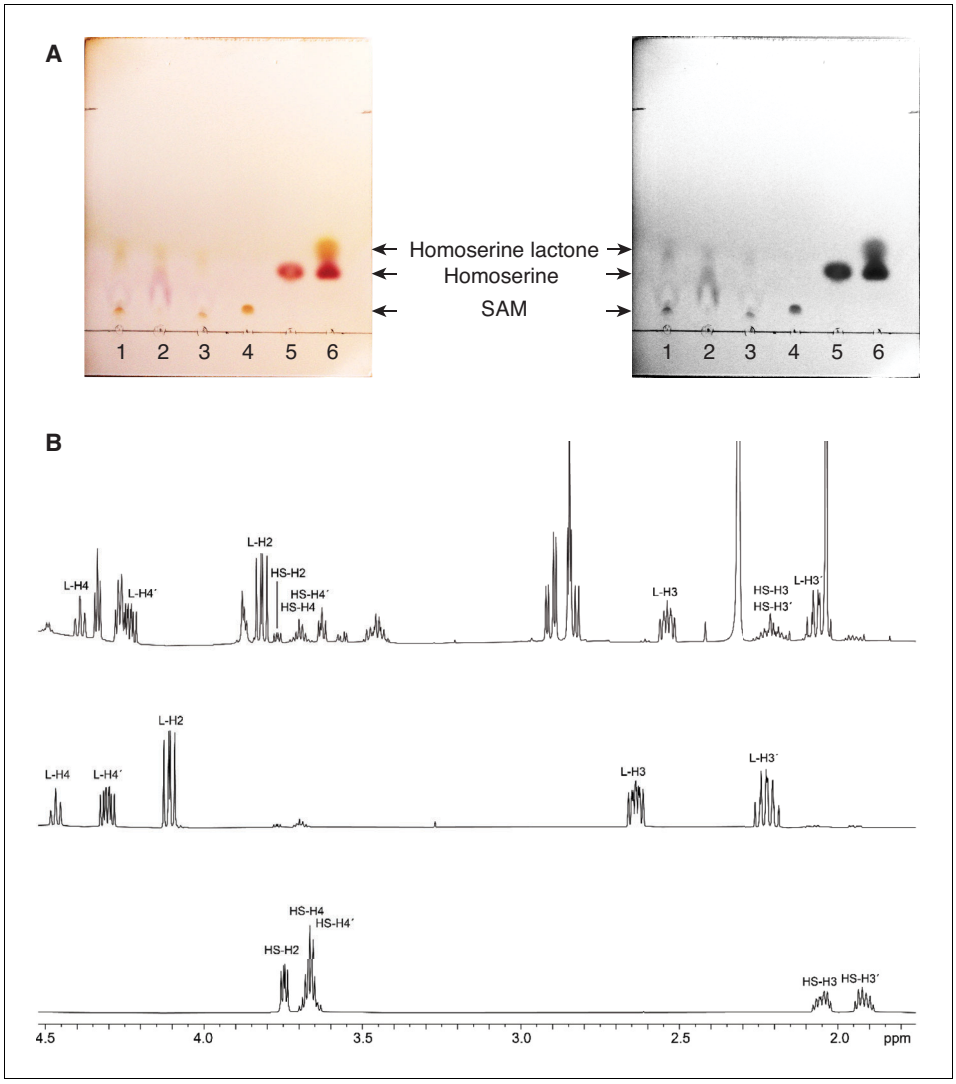

Figure 9. Characterization of SAMase reaction products. (**A**) TLC separation of enzymatic reactions and controls, shown in color and gray scale for clarity (1: Svi3-3, 2: T3 SAMase, 3: Orf1, 4: S-adenosyl methionine [SAM; 17 nmol], 5: L-homoserine [20 nmol], 6: L-homoserine lactone [400 nmol]). (**B**) ^{1}H nuclear magnetic resonance (NMR) spectra at 600 MHz in sodium phosphate buffer, D_2O, pH 7.4. Top: Enzymatic degradation of SAM (4 mM) (500 nM enzyme) after 45 min. Middle: Homoserine lactone (59 mM) showing onset of hydrolysis after 10 min. Bottom: Homoserine (57 mM).

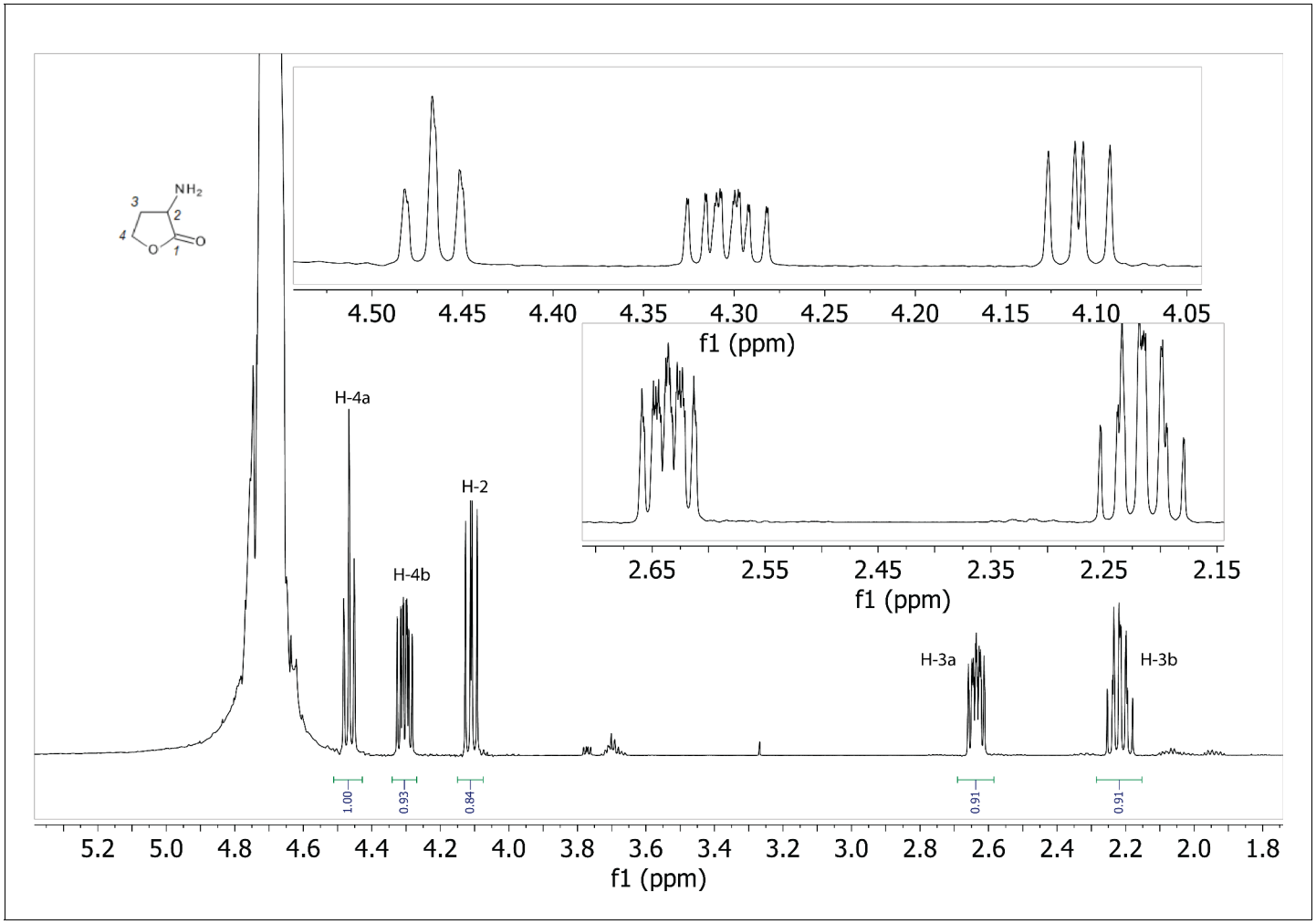

Figure 9—figure supplement 1. ^{1}H nuclear magnetic resonance (NMR) spectra of a reference sample of homoserine lactone (600 MHz, 59 mM in sodium phosphate buffer, D_2O, pH 7.4).

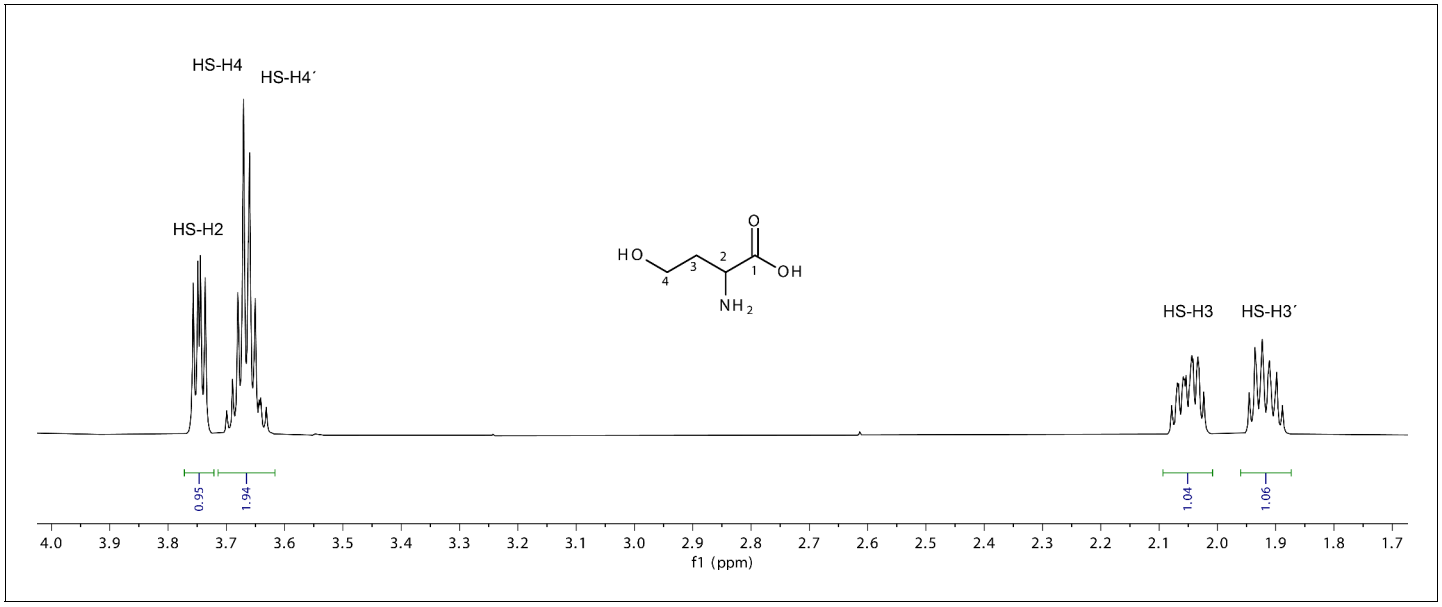

Figure 9—figure supplement 2. ^{1}H nuclear magnetic resonance (NMR) spectra of a reference sample of homoserine (600 MHz, 57 mM in sodium phosphate buffer, D_2O, pH 7.4).

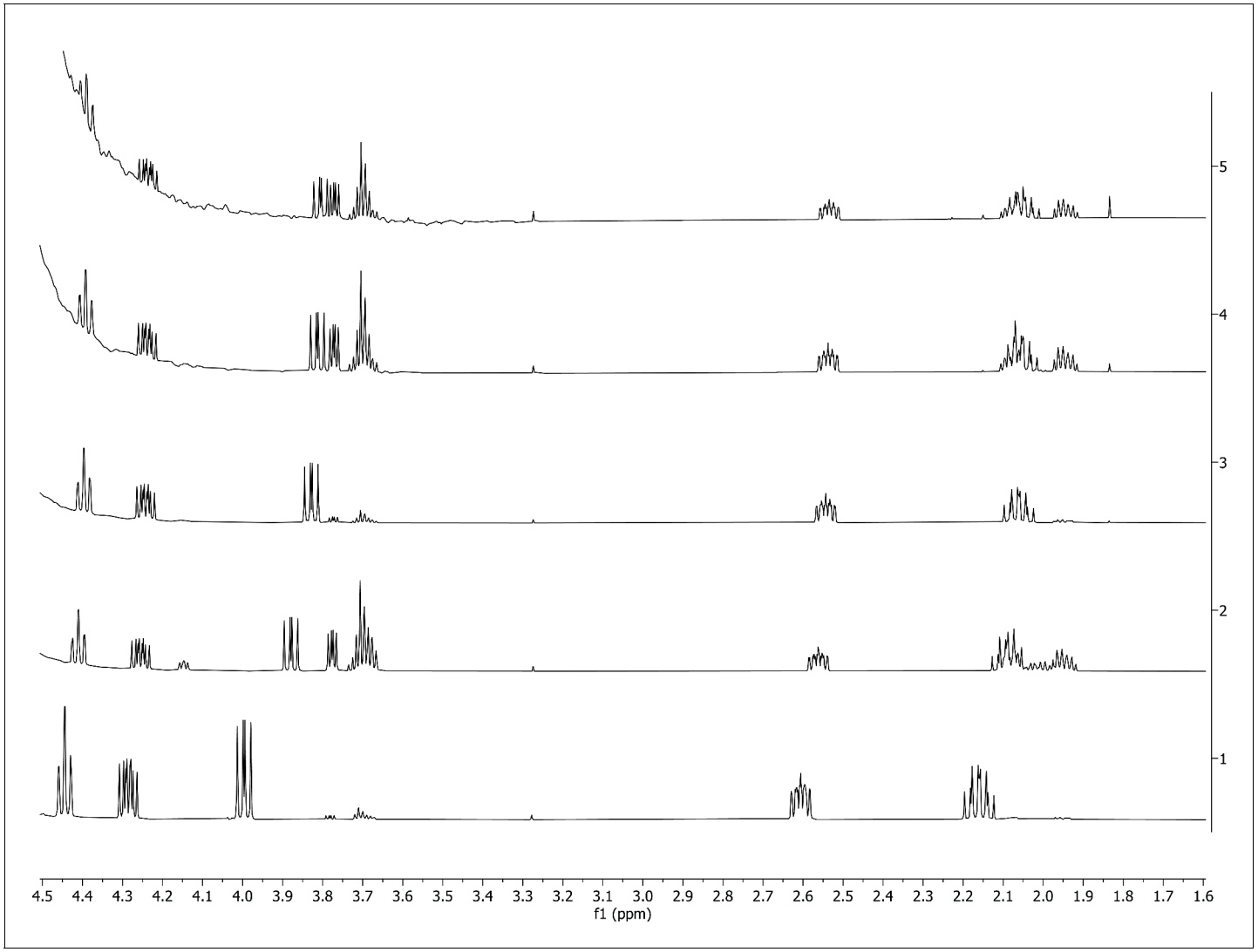

Figure 9—figure supplement 3. ^{1}H nuclear magnetic resonance (NMR) spectra of a reference sample of homoserine lactone at various concentrations and exposure times to sodium phosphate buffer showing progressive hydrolysis to homoserine (600 MHz, sodium phosphate buffer, D_2O, pH 7.4). Spectrum 1: 70 mM (t = 0); spectrum 2: 17.5 mM (t = 50 min); spectrum 3: 4.4 mM (t = 547 min); spectrum 4: 1.1 mM (t = 579 min); spectrum 5: 0.3 mM (t = 603 min).

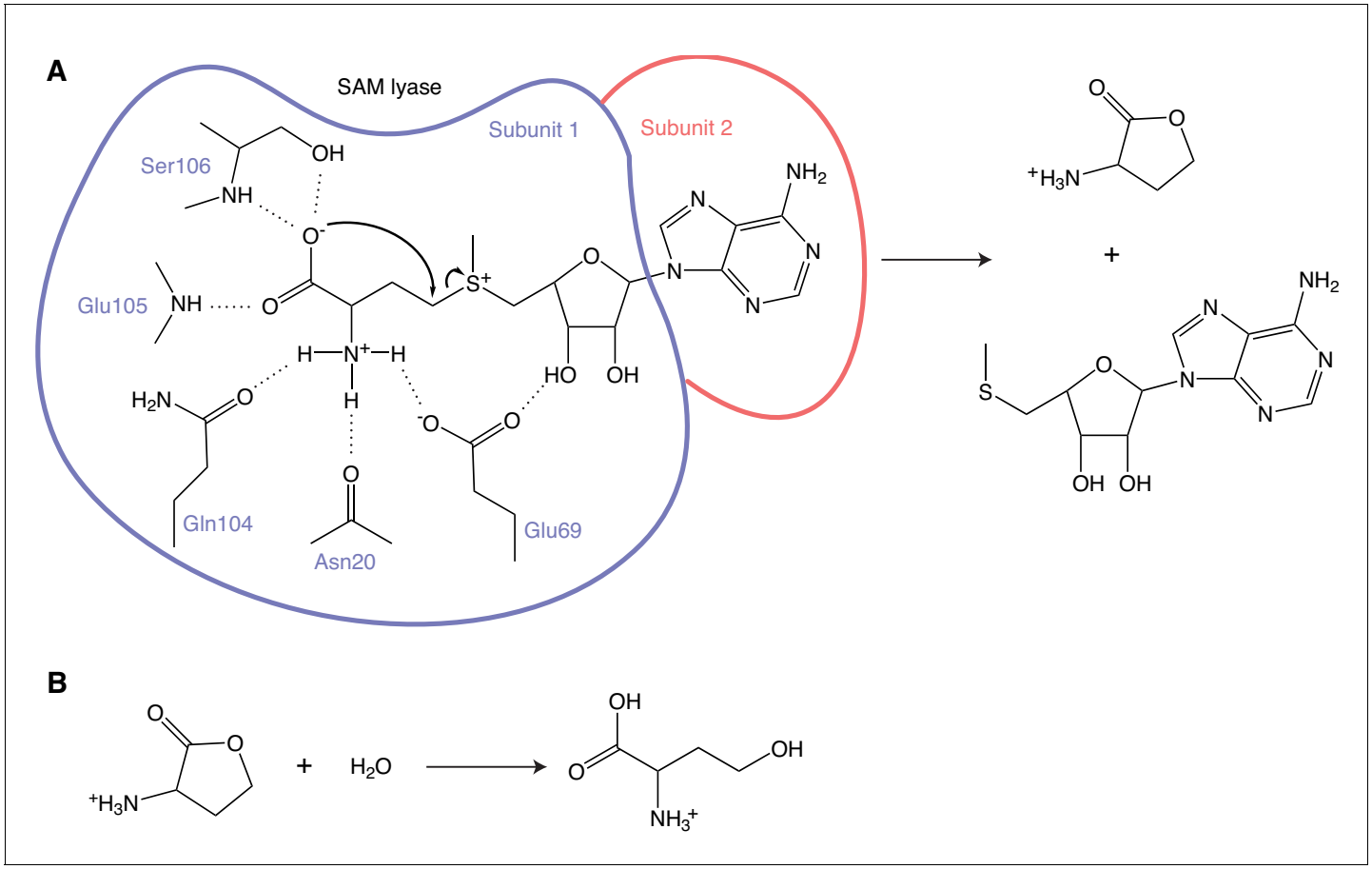

Figure 10. Mechanism of S-adenosyl methionine (SAM) degradation. (**A**) The first step is catalyzed by the SAM lyase, releasing the products homoserine lactone and 5'-methyl-thioadenosine (MTA). Hydrogen bonds between the enzyme and the reacting part of SAM are shown as dashed lines. The two subunits contributing to one active site are indicated in slate and salmon. (**B**) Homoserine lactone is spontaneously hydrolyzed to homoserine in solution.